



Integrated Project - EUWB

Contract No 215669

Deliverable

D8b.4

Channel model for complex automotive scenarios (in-car)

Contractual data:	M18
Actual data:	M19
Authors:	Stefan Gaier, Christiane Kuhnert, Andreas Waadt, Alex Viessmann, Guido Bruck, Shangbo Wang, Sebastian Rickers, Christoph Spiegel, Christian Kocks, Dong Xu, Mohammed Al-Olofi, Peter Jung
Participants:	BOSCH, UDE
Work package:	WP8
Security:	PU
Nature:	Report
Version:	1.0
Total number of pages:	21

Abstract

This document proposes a system model and software simulator for UWB channels in the EUWB automotive environment applications, as described in the deliverable D8b.1. The bases for the development of the channel model are field measurements in the automotive environment.

Keywords

Automotive, channel measurements, channel model, UWB.

Table of Contents

1 Executive summary	5
2 Introduction	6
3 Description of the mobile channel.....	8
3.1 Channel impulse response	8
4 Saleh Valenzuela model	10
4.1 Description and validity of the model	10
4.2 Large scale parameters	10
4.2.1 Deterministic channel attenuation	10
4.2.2 Stochastic channel attenuation with slow fading.....	11
4.2.3 Required large scale parameters.....	11
4.3 Small scale parameters	11
4.3.1 Stochastic description of the small scale parameters.....	11
4.3.2 Required small scale parameters	12
4.3.2.1 Instance of a PDP	12
5 Measurements in the automotive environment.....	14
6 Software simulator	16
7 Simulation results	18
8 Conclusion.....	20
References	21
Acknowledgement.....	21

List of Figures

Figure 3-1: Signals in the channel model of the equivalent lowpass band.....	8
Figure 4-1: Power delay profile of a Saleh Valenzuela channel with four clusters	12
Figure 5-1: Measurement in the automotive environment with a bi-conical antenna in front of the engine bonnet of a free standing car	14
Figure 5-2: Example of an antenna arrangement [9].....	14
Figure 6-1: Flow chart diagram of channel simulator	17
Figure 7-1: Example of a simulated channel impulse response	18
Figure 7-2: Fading leads to fluctuations in the channel energy.....	18
Figure 7-3: Averaged power decay profile.....	19

Abbreviations

EUWB	CoExisting Short Range Radio by Advanced Ultra-WideBand Radio Technology
MIMO	Multiple Input Multiple Output
PDP	Power Delay Profile
UWB	Ultra-WideBand

1 Executive summary

This document proposes a radio channel simulation for UWB channels in the EUWB automotive environment applications. It allows the generation of test channel impulse responses, which are used in software simulators.

Chapter 2 introduces the EUWB applications in the automotive environments and the resulting needs for the radio channel model.

Chapter 3 discusses the relevant fundamentals of mobile channel modes.

A certain channel model from Saleh and Valenzuela [3] is introduced in chapter 4. It is the basis of the utilized channel model and the implemented simulator.

Chapter 5 gives an overview about the conducted measurement campaigns, performed by BOSCH. A channel sounder is used to measure the mobile channel in the automotive environment in several test scenarios.

Chapter 6 discusses the developed software simulator.

Selected simulation results are given in chapter 7.

Chapter 8 concludes this report.

2 Introduction

Based on the open platforms, developed in work package WP7 of the EUWB project, the results of the work packages WP2 to WP6 shall be integrated into three different application environments. They are:

- public transport,
- automotive and
- home environment.

The development of applications requires detailed analysis of the coverage. For the planning of reliable wireless networks, link budget, bit error ratios (BER) and block error ratios (BLER) must be taken into account. Link budget calculations require the knowledge of the channel's large scale parameters, such as path attenuation and slow fading (cf. section 4.2). BER and BLER are usually derived from simulations, requiring detailed knowledge of the channel's small scale parameters, such as multi path propagation (cf. section 4.3). A model and simulation framework of the UWB mobile channel in the different application environments is therefore essential.

Requirements and system parameters of the UWB applications have been defined in [6],[7],[8] for environments in automotive, public transport, and home entertainment, respectively. Measurements and characterization of the mobile channel are conducted for all three of the application environments, before simulation frameworks are implemented. This report addresses the channel model for automotive environments. Channel models for the public transportation and home environment are investigated in WP8a and WP8c.

A realistic channel model for automotive must be based on field measurements in the automotive environment, taking the desired applications into account. The demonstration scenarios for automotive applications are described in [5]. There are three different functionalities, based on UWB technology, which will be investigated in the automotive applications cluster within the EUWB project. They are

- 1) localization of a dedicated tag,
- 2) detection and localization of passive non-cooperative objects, and
- 3) two-way data communication [5].

The dedicated tag to be localized is an active transmitter, which could for instance be integrated into a key fob. For its localization, it communicates with UWB receivers in the car's fixed infrastructure. Other applications examples are:

- door authorization with a range of 1-1.2 m,
- light dimming with a range of 2 m,
- individual seat position setup,
- entertainment and car system setup,
- climate control,
- intrusion sensing,
- occupancy sensing, for e.g. the seat belt pretensioner,

- remote connection of user interface elements to the body computer (“Remote UI”) and
- sensor to electronic control unit communication [5].

Setting out from the applications introduced in [5], several regions in the automotive environment can be distinguished [6]:

- passenger cabin,
- engine compartment, or
- outside the car at a distance of up to 2 m from the car body.

The collection of samples from mobile channels shall be performed in measurement campaigns. The frequency range of the UWB antennas shall be 6-9 GHz [6]. A channel sounder, collecting the samples, should therefore cover at least this frequency range 6-9 GHz.

Due to the small range of UWB, the amount of scattering obstacles in the automotive environment and the large bandwidth of several GHz, the multipath components (rays), observed by the receiver, will occur in clusters, formed by the multiple reflections from the objects in the vicinity of the UWB nodes. Furthermore, it can be assumed that Doppler is negligible due to the relative slow velocities in the mentioned automotive applications. Such mobile channel models have been described by Adel A.M. Saleh and Reinaldo A. Valenzuela in [3] after radio measurements in an indoor environment. In the Saleh Valenzuela channel model the clusters and multipath components within a cluster arrive according to Poisson processes. The inter-arrival times are exponentially distributed. The phase angles of the rays are independent uniformly distributed random variables $\varphi \in [0, 2\pi)$. The Saleh Valenzuela will be described in section 4 in more detail.

3 Description of the mobile channel

3.1 Channel impulse response

The mobile channel can be described by the channel impulse response $g(\tau, t)$. It describes the relation between the transmitted signal $s(t)$ at the input of the channel, and the signal at the channel's output. We assume that $s(t)$ is a bandpass signals

$$s(t) = \text{Re}\{u(t) \cdot e^{j2\pi f_0 t}\}, \quad (3.1)$$

with $u(t)$ being the equivalent lowpass signal of $s(t)$. In the following we will describe the mobile channel by the channel impulse response $h(\tau, t)$ in the equivalent lowpass band. With the generally time variant channel impulse response $h(\tau, t)$, the time t , and the path delay τ , the lowpass equivalent signal $v(t)$ at the channel's output becomes the time variant convolution

$$v(t) = \int_{-\infty}^{\infty} u(t - \tau) \cdot h(\tau, t) d\tau. \quad (3.2)$$

At the mobile receiver, noise $n(t)$ is added to the channel's output signal $v(t)$, yielding to the received signal

$$r(t) = v(t) + n(t). \quad (3.3)$$

Figure 3-1 illustrates the components and signals in the equivalent lowpass channel model.

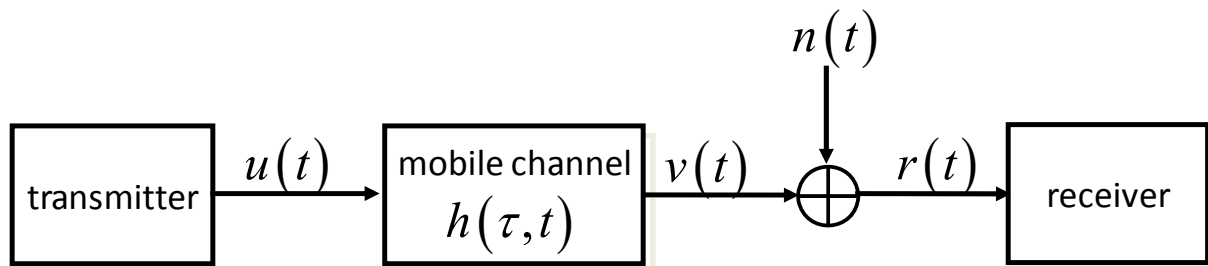


Figure 3-1: Signals in the channel model of the equivalent lowpass band

The signal $v(t)$ at the channel's output is a superposition of different representations of $u(t)$ with different path delay τ_i , different amplitudes, caused by different path gains β_i , and with different zero phase angles, caused by different phase shifts Θ_i of the channel's paths. Hence, $h(\tau, t)$ is often described by a generally infinite sum of shifted Dirac delta functions with different amplitudes and phase angles:

$$h(\tau, t) = \sum_{i=0}^{\infty} \beta_i(t) \cdot e^{j\Theta_i(t)} \delta(t - \tau_i(t)). \quad (3.4)$$

The channel impulse response $h(\tau, t)$ is generally time variant and changes with the time t , when mobile nodes, scatterers or obstacles move. However, if the relative velocities of the mobile nodes and all obstacles in the mobile channel are low, then the channel will change only slowly. In particular if the distance how far mobile nodes move between two adjacent transmitted bursts is small compared to the wavelength of the radio signal, then the mobile channel can be assumed to be virtually stationary [3], i.e. it is assumed to be time invariant between two adjacent bursts. This is often the case in indoor environments. The time invariant channel impulse response is independent of the time t :

$$h(t) = \sum_{i=0}^{\infty} \beta_i \cdot e^{j\Theta_i} \delta(t - \tau_i). \quad (3.5)$$

For the description of the mobile channel, a software channel simulator must generate triples of path gains β_i , phase angles Θ_i , and path delays τ_i in order to create channel impulse responses $h(t)$ according to (3.5). Due to the infinite calculation effort, it is not possible to generate infinite triples for the infinite sum of (3.5). The formula (3.5) is therefore approximated by a finite sum with K summands. K is sufficiently high, when the time difference of adjacent delays τ_i becomes smaller or equal to the system's time resolution, which is usually $1/B$, with B being the system bandwidth.

In order to generate the triples β_i , Θ_i , and τ_i , it is important to know about their stochastic properties. The phase angles Θ_i are statistically independent and equally distributed in the half open interval $[0, 2\pi)$. The path gains β_i and delays τ_i are small scale parameters and will be discussed in section 4.3.

Beside the interferences caused by the multipath propagation, (3.5) also describes the channel's attenuation A , or its reciprocal, the channel gain G . The channel gain is defined as the ratio between the signal's power P_{rx} at the channel's output to the signal's power P_{tx} at the channel's input. This ratio is a large scale parameter and can be calculated out of the path gains β_i to

$$G = \frac{P_{\text{rx}}}{P_{\text{tx}}} = \sum_{i=0}^{\infty} \beta_i^2 \quad (3.6)$$

As large scale parameters, channel gain and path loss will be described together with the shadowing model in section 4.2.

4 Saleh Valenzuela model

4.1 Description and validity of the model

Saleh and Valenzuela describe the mobile channel of a (indoor) office environment with clusters. The channel impulse response becomes the sum

$$h(t) = \sum_{l=0}^{\infty} \sum_{k=0}^{\infty} \beta_{kl} \cdot e^{j\Theta_{kl}} \delta(t - T_l - \tau_{kl}) \quad (4.1)$$

of impulse responses of the clusters, where the impulse response of every cluster can be described by (3.5) with a cluster delay T_l . l in (4.1) is the index of the $(l+1)$ -th cluster, whereas k is the index of the $(k+1)$ -th ray of the $(l+1)$ -th cluster [3].

4.2 Large scale parameters

4.2.1 Deterministic channel attenuation

The channel attenuation A is the ratio between the transmitted signal power P_{tx} at the channel's input to the signal's power P_{rx} at the channel's output. A is a random variable, which depends on the distance ρ between transmitter and receiver. The stochastic component of the attenuation is discussed in section 4.2.2. This section describes the relation between attenuation A and distance ρ without considering the stochastic component. In [3], A is described by an Okumura Hata model [4]. With the distance ρ in meters between transmitter and receiver, the attenuation becomes

$$A(\rho) = \frac{P_{tx}}{P_{rx}(\rho)} = A_0 \cdot \rho^\alpha, \quad (4.2)$$

where A_0 is the reference attenuation at $\rho = 1$ meter distance, and α is the attenuation exponent. Instead of the attenuation, one can also describe the overall channel gain

$$G(\rho) = \frac{P_{rx}(\rho)}{P_{tx}} = G(1) \cdot \rho^{-\alpha}, \quad (4.3)$$

being the reciprocal of $A(\rho)$. $G(1)$ in (4.3) is the reference channel gain at a distance of 1 meter. It will be shown in section 4.3 that the mean path magnitude $\overline{\beta_{00}^2}$ of the 1st ray from the 1st cluster can be calculated out of the overall channel gain to

$$\overline{\beta_{00}^2} = \frac{1}{\gamma \cdot \lambda} \cdot G(\rho), \quad (4.4)$$

with λ being the ray arrival rate and γ being the ray decay time. Both parameters, λ and γ , will be described in more detail in section 4.3. The ray arrival rate λ is the reciprocal of the mean delay value

between adjacent ray delays τ_{kl} . The ray decay time γ is the decay time with which the power delay profile of a cluster decays with increasing delay τ .

4.2.2 Stochastic channel attenuation with slow fading

The attenuation A is a lognormal distributed random variable. The logarithmic attenuation

$$a / \text{dB} = 10 \cdot \log_{10}(A) \quad (4.5)$$

is Gaussian distributed. With the standard deviation σ_a of a , and with the mean logarithmic attenuation

$$\overline{a(\rho)} / \text{dB} = a_0 + 10 \cdot \alpha \cdot \log_{10}(\rho), \quad (4.6)$$

with a_0 being the mean logarithmic reference attenuation in dB at a distance of $\rho = 1$ meter, a sample of the actual attenuation becomes

$$a(\rho) = \overline{a(\rho)} + \xi. \quad (4.7)$$

$\xi \in \mathcal{N}(0, \sigma_a)$ in (4.7) is a normal distributed random variable with mean value $\overline{\xi} = 0$ and standard deviation $\sqrt{\overline{\xi^2}} = \sigma_a$. (4.7) takes the stochastic nature of the attenuation into account.

4.2.3 Required large scale parameters

The following parameters are required to describe the channel attenuation or the overall channel gain respectively:

- a_0 , the mean channel attenuation from (4.6) in dB at a reference distance of $\rho = 1$ meter,
- α , the attenuation exponent in (4.6), and
- σ_a , the logarithmic standard deviation of the lognormal distributed attenuation in (4.7).

4.3 Small scale parameters

4.3.1 Stochastic description of the small scale parameters

For the synthesis of channel impulse responses according to (4.1), quadruples of the small scale parameters T_l (cluster delay), τ_{kl} , (ray delay), β_{kl} (ray gain), and Θ_{kl} (phase angle) must be created. The phase angles Θ_i are statistically independent and equally distributed in the half open interval $[0, 2\pi)$ and can therefore be created out of equally distributed, statistically independent random variables. The creation of the cluster delays T_l , the ray delays τ_{kl} , and the ray gains β_{kl} will be discussed in section 6. This creation is done on the basis of only few characteristic key parameters.

The key parameters, describing the stochastic properties of the channel, can be used to synthesize the triples T_l , τ_{kl} , and β_{kl} , and therefore the channel impulse response from (4.1). They can be found

after measurements of the power delay profiles (PDP) of the mobile channel, and are described in section 4.3.2.

4.3.2 Required small scale parameters

4.3.2.1 Instance of a PDP

The following parameters are required to describe the power delay profile (PDP) and the stochastic properties of the channel in small scale:

- γ , the ray decay time,
- Γ , the cluster decay time,
- Λ , the cluster arrival rate,
- λ , the ray arrival rate.

They can be found after measurements of the power delay profiles (PDP) of the mobile channel. Figure 4-1 shows an example of a PDP for a Saleh Valenzuela channel with $L = 4$ clusters. For $L = \infty$ clusters, the PDP can generally be written as

$$\overline{\beta^2(\tau)} = \overline{\beta_{00}^2} \cdot \sum_{l=0}^{\infty} e^{-T_l/\Gamma} e^{-(\tau-T_l)/\gamma} U(\tau-T_l), \quad (4.8)$$

with the ray gain β_{00} of the 1st ray in the 1st cluster, the delay T_l of the $(l-1)$ th cluster, the cluster decay time Γ , the ray decay time γ , and with the Heaviside step function $U(\tau)$.

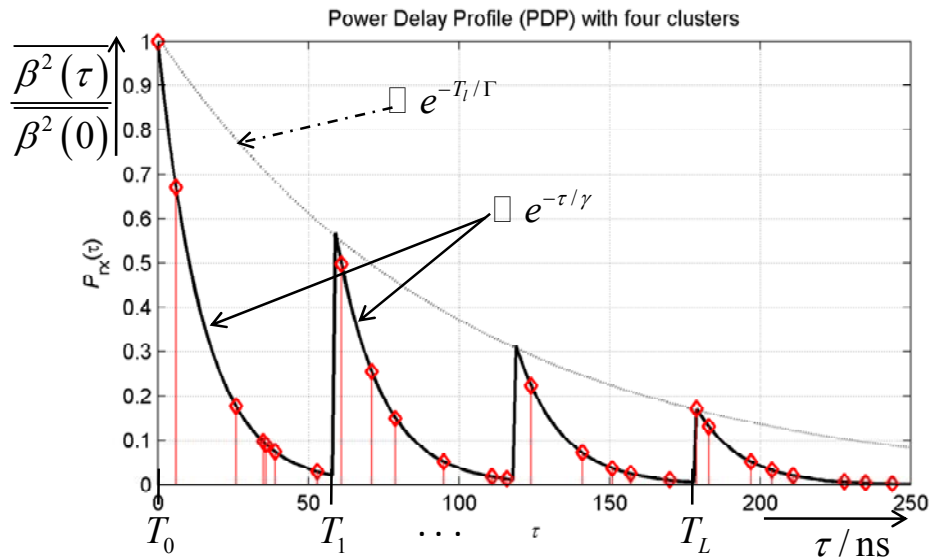


Figure 4-1: Power delay profile of a Saleh Valenzuela channel with four clusters

The cluster delays of the $L = 4$ shown clusters in the PDP in Figure 4-1 are $T_0 = 0$, $T_1 = 60$ ns, $T_2 = 120$ ns, and $T_3 = 180$ ns. The average delay difference of two adjacent clusters is 60 ns, yielding to a cluster arrival rate of $\Lambda = 1/60 \text{ ns} = 1,67 \cdot 10^7 \text{ s}^{-1}$.

Every cluster decays proportionally to $e^{-\tau/\gamma}$, with a ray decay time of $\gamma = 15 \text{ ns}$.

The amplitude of the clusters decays proportionally to $e^{-T_i/\Gamma}$, with a cluster decay time of $\Gamma = 100 \text{ ns}$.

The red markers in Figure 4-1 show single received rays or samples of the PDP. The average delay difference between adjacent rays is 10 ns, yielding to a ray arrival rate of $\lambda = 1/10 \text{ ns} = 1 \cdot 10^8 \text{ s}^{-1}$.

5 Measurements in the automotive environment

For the three UWB based functionalities in the automotive scenarios, measurements were performed at the premises of the EUWB partner BOSCH.

Measurements were carried out in different antenna arrangement scenarios with three types of antennas: bi-conical, Vivaldi and with monopole antennas. Figure 5-1 shows a measurement example with a bi-conical antenna in front of the engine bonnet of a free standing car.



Figure 5-1: Measurement in the automotive environment with a bi-conical antenna in front of the engine bonnet of a free standing car

Figure 5-2 shows an example of an antenna arrangement scenario. The green points in Figure 5-2 illustrate the fixed anchor nodes of the car's infrastructure. The red points are the mobile nodes or tags. The measurements were carried out with the car standing free, in a garage or in a parking spot.

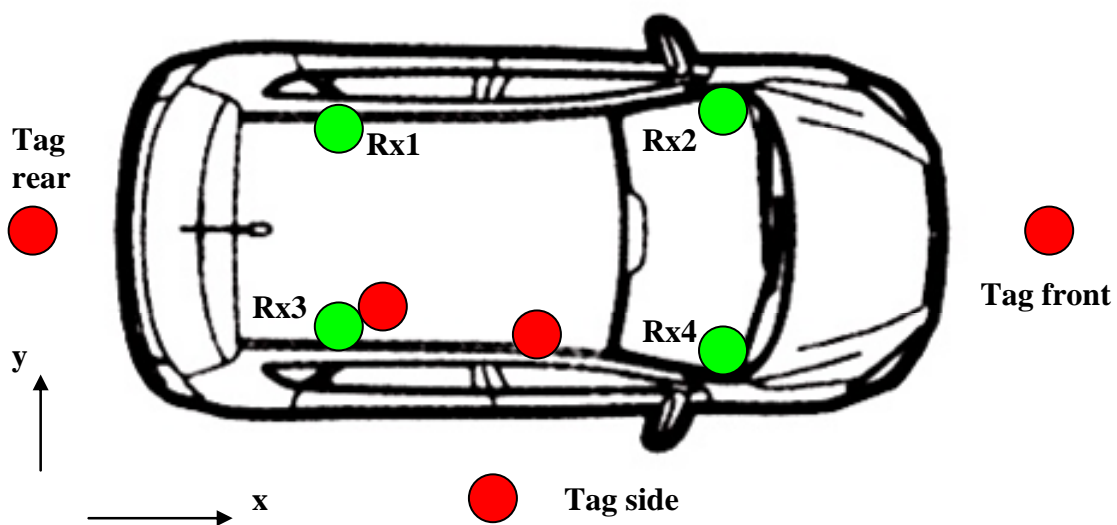


Figure 5-2: Example of an antenna arrangement [9]

A detailed description of the measurement scenarios is given in [9].

The outcome of the measurement campaigns are Matlab files with samples of channel impulse responses, which were collected with a channel sounder. The calibrated data can be loaded from the Matlab files with the “load *filename* –mat” command.

6 Software simulator

The flow chart diagram of the channel simulator software is depicted in Figure 6-1. First the model parameters are loaded in the initialization phase. They are the cluster arrival rate Λ , ray arrival rate λ , cluster decay time Γ , ray decay time γ and standard deviations σ_a , σ_c , σ_r of the fading. σ_a is the standard deviation of the log-normal variable for the slow shadow fading, σ_c is the standard deviation of the log-normal variable for cluster fading, and σ_r represents the ray fading. The model parameters must be derived from field measurements.

After loading the model parameters, the cluster arrival time t_c , the ray arrival time t_r are initialized as well as their counters c and r . The initialization of the cluster parameters c and t_c is done only once per simulated channel impulse response, whereas the ray parameters r and t_r are initialized to zero at the beginning of every cluster. The outer loop in Figure 6-1 is the loop over the clusters of the channel impulse response. The inner loop is the loop over the rays within a cluster. In the inner loop, the points in time $\tau_{c,r}$ of arriving rays and the amplitudes β of these rays are determined. The ray phase $\Theta_{c,r}$ is set to an equally distributed random variable χ in the interval $[0, 2\pi)$. At the end of the loop over rays, the ray arrival time is updated and increased by an exponentially distributed random variable $E(\lambda)$ with mean value λ . The inner loop is terminated, when the ray arrival time exceeds a certain threshold, here set to the decuple of the ray arrival rate λ .

After determining the amplitudes and phases of all rays within a cluster, the cluster arrival time is updated and increased by an exponentially distributed random variable $E(\Lambda)$ with mean value Λ . The outer loop is terminated, when the cluster arrival time exceeds a certain threshold, here set to the decuple of the cluster arrival rate Λ . When the amplitudes and phases of all rays in all clusters have been determined, the channel impulse response can be composed according to (4.1).

The simulator has been implemented in Matlab and in C with mex interfaces to Matlab.

For the validation of the statistics of the generated channel impulse responses, the described process is repeated many times to generate a stochastically meaningful set of channel impulse responses. Then the mean channel energy and fading can be analyzed.

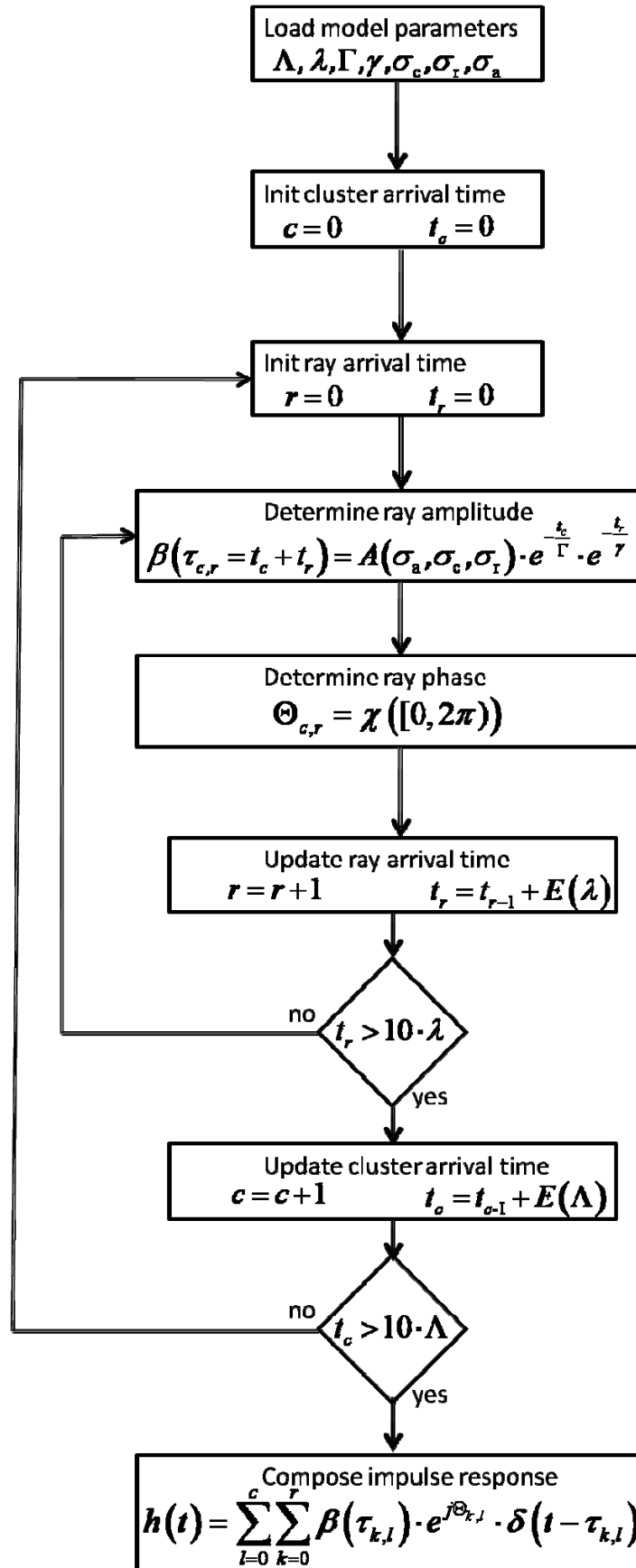


Figure 6-1: Flow chart diagram of channel simulator

7 Simulation results

Figure 7-1 shows a realization of a simulated channel impulse response $h(t)$. The absolute value of h is charted over the delay.

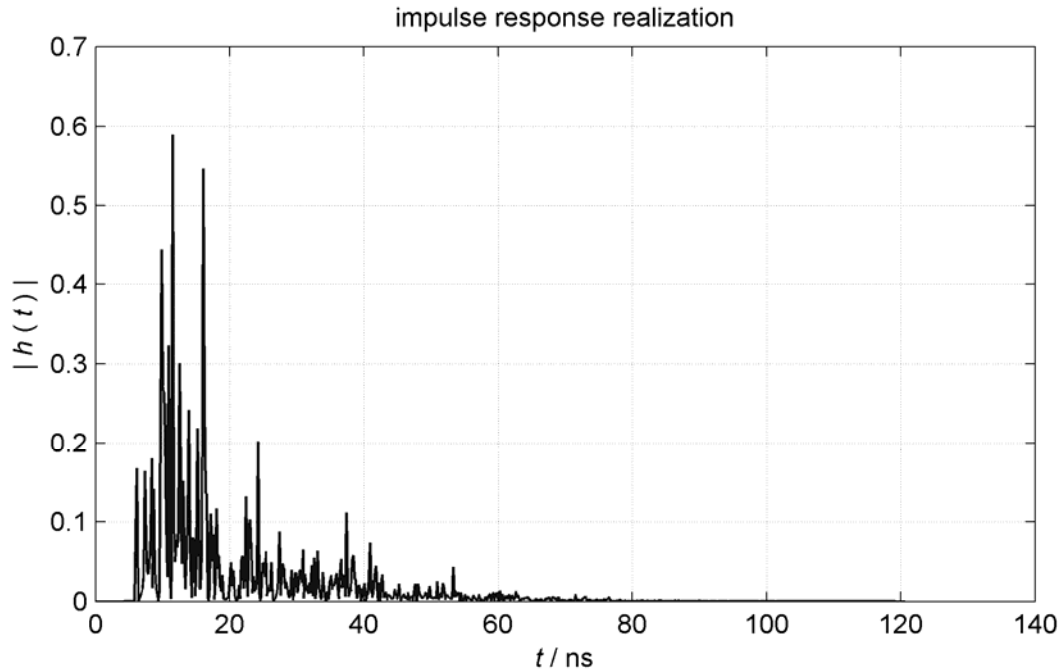


Figure 7-1: Example of a simulated channel impulse response

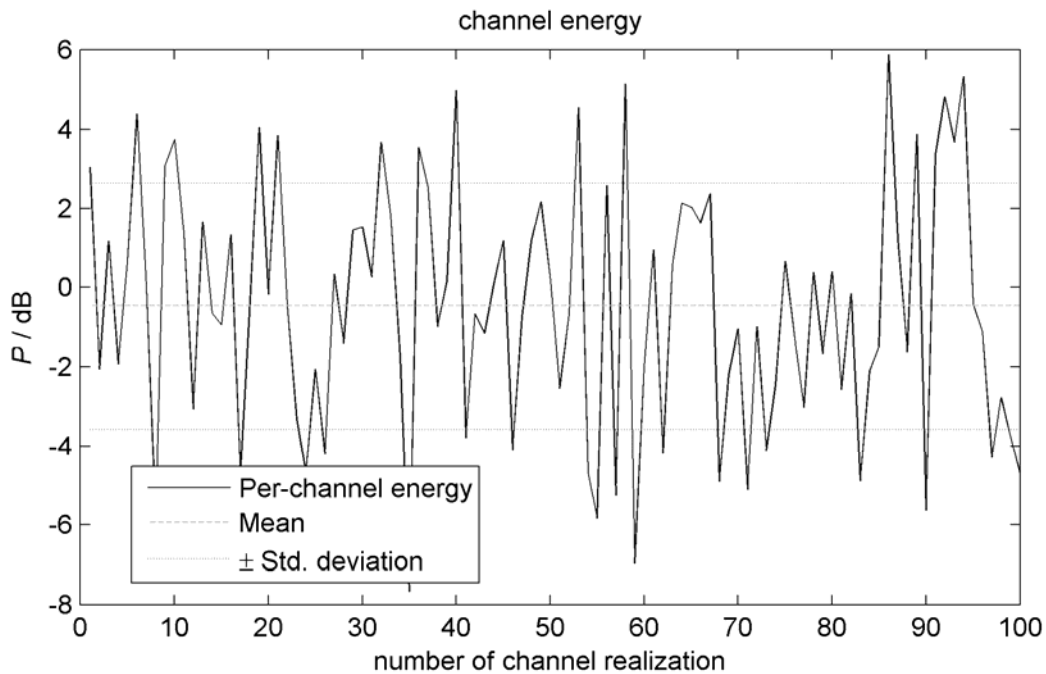


Figure 7-2: Fading leads to fluctuations in the channel energy

The simulations include fading in the amplitudes of h . Figure 7-2 shows the resulting channel energy, fluctuating with a standard deviation of about 3.4 dB around a mean energy value.

The averaged power delay profile is depicted in Figure 7-3. The thin gray dashed line shows the average from two channel impulse responses. The average from 100 channel impulse responses is illustrated by the black continuous line.

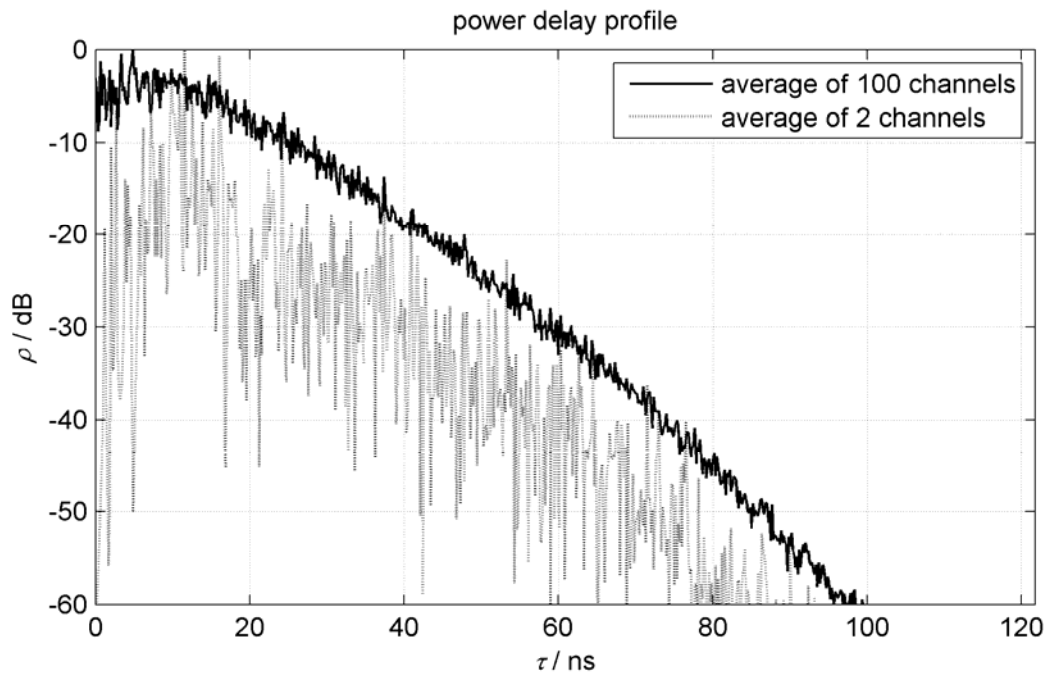


Figure 7-3: Averaged power decay profile

8 Conclusion

A software simulator for generation of channel impulse responses of the mobile UWB channel has been developed and implemented. The ratio simulator is based on a Saleh Valenzuela model. The simulated channel is defined by model parameters such as arrival rates λ , and decay times γ . The values of these parameters must be extracted from measurement data, gathered during measurement campaigns in the automotive environment. The measurement campaigns were carried out by BOSCH in several defined measurement scenarios, adjusted to the planned automotive applications. The extraction of the mentioned model parameters is under progress.

References

- [1] Zeisberg, S., Schreiber, V.: “EUWB - Coexisting Short Range Radio by Advanced Ultra-Wideband RadioTechnology”, ICT Mobile and Wireless Communications Summit, Stockholm, June 2008, accepted for publication
- [2] URL of EUWB consortium: <http://www.euwb.eu>
- [3] A. Saleh, and R. Valenzuela, “A Statistical Model for Indoor Multipath Propagation”, *IEEE journal on selected areas in communications*, vol. SAC-2, no. 2, Feb. 1987, pp. 128–137.
- [4] Y. Okumura, E. Ohmori, T. Kawano, and K. Fukuda, "Field Strength and Its Variability in VHF and UHF Land-Mobile Radio Service," *Review of the Electrical Communication Laboratory*, vol. 16, pp. 825-873, September-October, 1968.
- [5] J. Hasch, “Scenario description for automotive environment applications”, Deliverable D8b.1 of the Integrated Project – EUWB, June 2008.
- [6] J. Hasch, “System parameters for automotive environment applications”, Deliverable D8b.2 of the Integrated Project – EUWB, December 2008.
- [7] S. Bovelli, F. Leipold, “Requirements for public transport applications”, Deliverable D8a.2 of the Integrated Project – EUWB, October 2008.
- [8] P. Hafezi, M. Rey, “System Parameters and Technical Requirements for Multiband/Multimode UWB Home Environment Applications”, Deliverable D8c.2 of the Integrated Project – EUWB, October 2008.
- [9] R. Zetik, A.P.G. Ariza, R. Thomä, W. Kotterman, “Application-specific MIMO-UWB channel measurements and parameter extraction (final)”, Deliverable D3.1.2b of the Integrated Project – EUWB, August 2009.

Acknowledgement

The EUWB consortium would like to acknowledge the support of the European Commission partly funding the EUWB project under Grant Agreement FP7-ICT-215669 [1],[2].